Journal of Photochemistry and Photobiology A: Chemistry 221 (2011) 130–137

Contents lists available at ScienceDirect

Journal of Photochemistry and Photobiology A: Chemistry

journal homepage: www.elsevier.com/locate/jphotochem

Review

# Photochemical reaction fields with strong coupling between a photon and a molecule

Kosei Ueno [a,b], Hiroaki Misawa [a,*]

[a] Research Institute for Electronic Science, Hokkaido University, Sapporo 001-0021, Japan
[b] PRESTO, Japan Science and Technology Agency, Kawaguchi 332-0012, Japan

ARTICLE INFO

*Article history:*
Available online 19 April 2011

*Keywords:*
Plasmon photochemistry
Strong coupling between a photon and a molecule
Photoelectric conversion
Gold nanoblocks

ABSTRACT

To achieve a future low-carbon society, the effective utilization of photons is essential for the development of technologies based on photochemistry, such as photocatalysis and dye-sensitized solar cells, which have the potential to produce clean energy as well as preserve the environment. Here, we propose that gold nanostructures exhibiting localized surface plasmon (LSP) resonance are promising sites for photochemical reaction fields that increase the interaction between a photon and molecule. These interactions are based on electromagnetic field enhancement effects that are induced by LSP excitations and their localization. In this review, recent studies on the strong coupling field between a photon and molecule for photochemical reactions are discussed. As an outstanding example, this concept was applied to the plasmonic, photoelectric conversion of visible to near-infrared wavelengths using electrodes in which gold nanoblocks were elaborately arrayed on the surface of a single $TiO_2$ crystal. The most important characteristic of this photoelectric conversion is that the photocurrent was stable for more than 200 h without adding the donors, which suggests the possibility that water molecules can act as donors that provide electrons to the d-band holes assisted by the LSP excitation. Therefore, this system has the potential for use in artificial photosynthesis systems with irradiation from near-infrared light.
© 2011 Elsevier B.V. All rights reserved.

## 1. Introduction

Photochemistry plays an essential role in the development of photoscience and technology. Photolithography [1,2], bio-imaging techniques [3,4], photosynthesis [5,6], photocatalysis [7,8], and dye-sensitized solar cells [9,10] are based on the principles of photochemistry. Thus far, the light absorption process has not been intensively examined. Rather, research has focused mainly on the excited-stated molecules after the light absorption process and their subsequent chemical reactions, such as electron transfer [11,12] and energy transfer [13,14]. The concept of quantum efficiency describes the probability of a photochemical reaction involving the excited-state molecules following the light absorption process; however, the interaction between photons and molecules is not very strong. The probability of interaction between a photon and a molecule can be roughly estimated at $10^{-7}$ because the focal spot size of the light is $10^7$ times larger than the general molecular absorption cross-section due to the relationship between the diffraction limit of the incident light and the size of the molecule. Thus far, the number of excited-state molecules has been increased by increasing photon density using a laser as the excitation source. However, there is a loss of energy because the probability of interaction does not change. In the case of a total system, such as a solar cell, the importance of the light absorption process is readily apparent in photochemical research.

Recently, it was reported that metallic nanostructures exhibiting localized surface plasmons (LSPs) are promising in photochemical reaction fields [15–18]. These structures allow the interaction between photons and molecules to be enhanced. Recently, a significant photopolymerization reaction was reported to occur via two-photon absorption in the photoinitiator molecules of negative photoresists in the nanogaps of closely spaced gold nanoparticles irradiated by a weak incoherent light source, such as a halogen lamp [15]. The photochemical reaction fields use the localization of electromagnetic waves within nanogaps to overcome the diffraction limit of light [19]. Thus, gold nanostructures are useful in photochemical reaction fields, by enabling the promotion of strong coupling between photons and molecules that in turn enhance the effective use of photons. From this standpoint, the concept of effective photon usage can be applied to a plasmonic photoelectric conversion system that responds to wide ranges of solar light wavelengths [20].

The development of a high-efficiency solar cell is essential for the development of a low-carbon society. To construct a solar cell with high photoelectric conversion efficiency, a system that responds to a wide spectrum of solar light from visible to near-

* Corresponding author. Tel.: +81 11 706 9358; fax: +81 11 706 9359.
*E-mail address:* misawa@es.hokudai.ac.jp (H. Misawa).

1010-6030/$ – see front matter © 2011 Elsevier B.V. All rights reserved.
doi:10.1016/j.jphotochem.2011.04.014

infrared wavelengths is necessary. However, the photoelectric conversion properties of the amorphous silicon solar cells commonly used today are known to drastically decrease in wavelength ranges longer than 700 nm [21]. For photoelectric conversion at wavelengths longer than 800 nm, a dye sensitized solar cell with a particulate titanium dioxide ($TiO_2$) electrode covered with sensitizers, such as metal complexes and gold nanoparticles, has been suggested [22,23]. However, the spectral distribution in the infrared wavelength region above 800 nm corresponds to ~40% of the entire solar energy on earth, and only a few solar cells can efficiently convert solar energy with these longer wavelengths to electrical energy. Recently, the plasmonic, photoelectric conversion from visible to near-infrared wavelengths was successfully demonstrated using electrodes in which gold nanoblocks were elaborately arrayed on the surface of $TiO_2$ single-crystal electrodes via a top-down nanostructuring process. In this system, the generation of larger photocurrent was attained from the optical antenna effects on the gold nanorods. Interestingly, this photoelectric conversion system can be used as a solar cell that can be embedded in living tissue because it is able to use light with wavelengths from 800 to 1200 nm, which is the absorbing spectral window for biological systems.

In this review, recent studies concerning the construction of a strong coupling field between a photon and molecule for photochemical reactions and effective photon usage are discussed. First, the fabrication of metallic nanostructures exhibiting LSP resonances and their spectral and optical properties are described. Next, research studies are discussed that use surface-enhanced Raman scattering (SERS) to evaluate electromagnetic field enhancement effects localized on the fabricated metallic nanostructures, which leads to strong coupling between a photon and a molecule. Finally, studies are described that explore plasmon-assisted photochemical reactions using two-photon photopolymerization, including research on plasmonic photocurrent generation from visible to near-infrared wavelengths, and the significance of strong coupling fields between a photon and a molecule in the context of a photochemical reaction is discussed.

## 2. Fabrication of metallic nanostructures showing LSP and their optical properties

Various sizes and shapes of metallic nanoparticles exhibiting LSP have been chemically synthesized [24–30]. Gwo et al. have demonstrated control of the gap width of two diagonally aligned metallic nanocrystals, which were chemically synthesized with nanometric accuracy, according to controlling the position of the nanocrystals with mechanical probes equipped with a scanning electron microscope (SEM) system. Elucidation of the optical properties of the crystals indicates the existence of bright and dark plasmon modes [31]. However, controlling the arrangements of chemically produced metallic nanoparticles on solid substrates remains difficult. Advanced nanoprocessing methods using high resolution electron beam lithography (EBL) allow for the fabrication of metallic nanostructures with nanometric accuracy, while their arrangement on a substrate may be achieved more easily [32–35].

As one example of these fabrication methods, our fabrication technique was implemented as described here. Planar patterns of gold nanoblocks were fabricated on glass substrates (Matsunami Co., Japan) in an area of 24 mm × 24 mm using high-resolution electron beam lithography (ELS-7700H, Elionix Co., Ltd., Japan) that was operated at 100 kV accelerating voltage. A co-polymer resist (ZEP-520a, Zeon Co., Ltd., Tokyo, Japan) diluted with ZEP thinner (1:1) was spin-coated on the substrates at 1000 rpm for 10 s and at 4000 rpm for 90 s. After pre-baking on a hot plate for 3 min at 180 °C, EBL was carried out at an electrical current of 5 pA. After developing using a standard developer (Zeon Co., Ltd., Japan), a 2 nm chromium and 40 nm gold bilayer was deposited by sputtering (ULVAC, MPS-4000, Japan). Then, lift-off was performed by immersing the fabricated sample in acetone solution (Wako Pure Chemical Industrials Ltd., GR Grade) in an ultrasonic bath for 2 min and then in a resist remover (Zeon Co., Ltd., Tokyo, Japan) for 2 min [36–38].

To elucidate the resolution of our fabrication methods, patterns were prepared that had a rectangular footprint of dimensions $(w = 143 \pm 3.3) \times (l = 373 \pm 2.7 + \Delta l)\,\mathrm{nm}^2$, where $\Delta l = N \times 1.93 \pm 0.38$ nm ($N = 0$, 2.14) is the block length increment in the fabricated set of 15 samples. Nanoblocks with a design height of $h = 30$ nm were fabricated using a lift-off technique on a 2 nm Cr buffer layer to achieve better adhesion. The significant advantage of this technique over chemical synthesis is the potential to obtain large ensembles of identically oriented nanoblocks. Fig. 1(a) shows a SEM image of the nanoblocks with $N = 0$. Fig. 1(b) presents the schematic parameters of the nanoblocks. The elongated shape of the nanorods distinguishes the longitudinal (L) versus transverse (T) surface plasmon modes associated with these nanoparticles [39–42]. Longitudinal and transverse modes can be excited in the entire ensemble by radiation polarized linearly along the direction parallel to the longer and shorter axes of the blocks, respectively, as shown in Fig. 1(b). The length of the nanoblocks was chosen to tune their longitudinal plasmon mode; the properties of this mode are very important to this work. An appropriately large separation between the blocks of 200 nm was chosen to prevent significant dipole–dipole coupling [43–47].

Fig. 1(c) presents optical extinction spectra for the samples under L-mode excitation conditions. An area of 10 μm × 10 μm comprising 312 nanoblocks was imaged on each sample. According to classical Maxwell electrodynamics, the peak wavelengths of these modes should roughly scale with the corresponding dimensions of the nanoblocks [48–50]. As expected, the extinction peaks in L mode exhibit a monotonous and pronounced red-shift with the increasing design length of the blocks, but the peaks in T mode are almost identical across all of the samples because their transverse size is the same. The spectral positions of the extinction peaks are summarized in Fig. 1(d). It is noteworthy that an increase in the block length by a single step, which means $\Delta l$ when $N = 1$, yields an easily detectable spectral shift of the peak by about 5 nm. Thus, the above data demonstrate the high sensitivity of the longitudinal plasmon resonance to the design length of the nanoblocks. This result means that block length can be determined with an accuracy corresponding to the thickness of about ~4–12 atomic gold layers, which can be prepared using recently developed nanoprocessing methods [51].

### 2.1. Electromagnetic field enhancement effects on SERS from gold nanoblocks

LSPs are associated with electromagnetic (EM) field enhancement effects [52–57]. Various optical effects, such as non-linear electronic excitation [58,59], higher order harmonic generation [60,61], and surface-enhanced Raman scattering (SERS) [62–65], are promoted in the vicinity of metallic nanoparticles due to EM field enhancement effects. Itoh and co-workers demonstrated EM field enhancement effects on SERS by measuring SERS signals from single silver nanoparticle pairs and analyzing the data according to EM theory on SERS [66]. Based on EM theory on SERS, SERS intensity is related to plasmonic enhancement effects at the wavelengths of both incident light field and scattering light fields according to the following equation [67]:

$$P_s(\nu_s) = N\sigma_{\mathrm{SERS}} L(\nu_i)^2 L(\nu_s)^2 I(\nu_i), \quad (1)$$

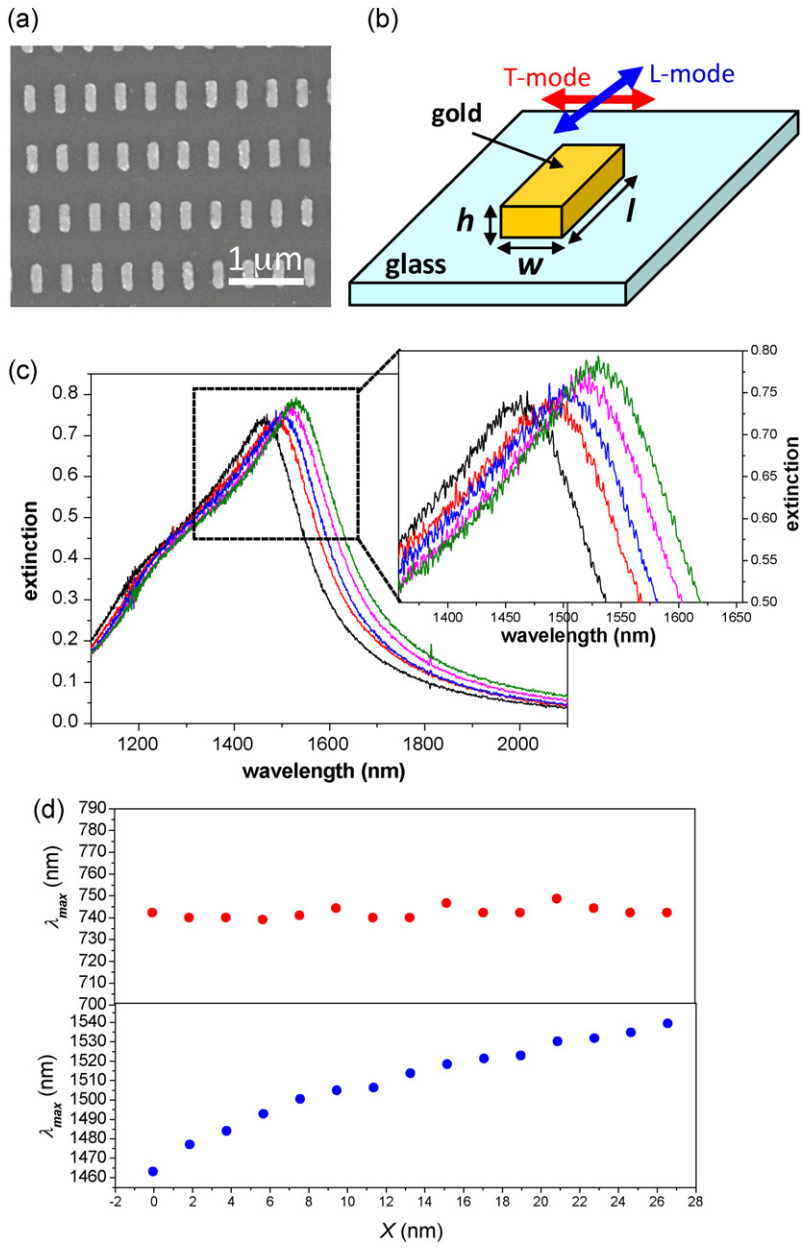


**Fig. 1.** (a) A scanning electron microscope (SEM) image of the gold nanoblock sample with $N = 0$. (b) A schematic drawing of the nanoblock on a glass substrate with explanation of nanoblock dimensions and directions of linear polarization required for the excitation of L and T modes of the LSP. (c) Polarized extinction spectra measured in ensembles of 312 nanoblocks with different lengths $l$, with $N = 0$, 3, 5, 8, 11, and 14. (d) The spectral position of the extinction peaks of transverse (upper) and longitudinal (lower) modes versus $\Delta l$.

where $L(\nu_i)^2$ is the enhancement factor at the wavelength of incident light ($L(\nu_i) = |E_{loc}(\nu_i)| / |E(\nu_0)|$), and $L(\nu_s)^2$ is the enhancement factor at the Raman scattering wavelength ($L(\nu_s) = |E_{loc}(\nu_s)| / |E(\nu_0)|$). Additionally, $N$ is the number of molecules contributing to SERS signals, $\sigma_{SERS}$ is the Raman scattering cross-section that includes chemical effects on SERS (as determined by the type of molecule), and $I(\nu_i)$ is the incident laser power in the SERS measurement. Therefore, it is expected that SERS intensity is affected by the extinction values of the plasmon resonance band at the wavelengths of both incident light and scattered light.

The relationship between SERS intensity and the extinction value for both light wavelength types was analyzed in detail. Well-defined gold nanoblocks of various sizes were fabricated, and detailed surface-enhanced Raman scattering (SERS) properties of crystal violet molecules were then studied. SEM images of gold nanoblocks fabricated on glass substrates are shown in Fig. 2(a) and (b). In the present study, the side length of the nanoblock (that is, $l$ and $w$) and the interval distance between gold nanoblocks were set at identical values ranging from 80 nm to 180 nm. As shown in Fig. 2(a) and (b), gold nanoblocks of size 90 nm × 90 nm × 25 nm (a) and 160 nm × 160 nm × 25 nm (b) were constructed. Fig. 2(c) presents extinction spectra for gold nanoblocks with various side lengths; the extinction spectra exhibit red shift as the size of the gold nanoblocks increased.

SERS spectra of crystal violet molecules with several nanoblock sizes are shown in Fig. 2(d). The spectral bands identified at about 913, 1173, and 1383 $cm^{-1}$ in these SERS spectra (Fig. 2(d)) are attributed to the ring skeletal vibrations in the radical orientation, ring C–H out-of-plane bending, and N-phenyl stretching vibrations

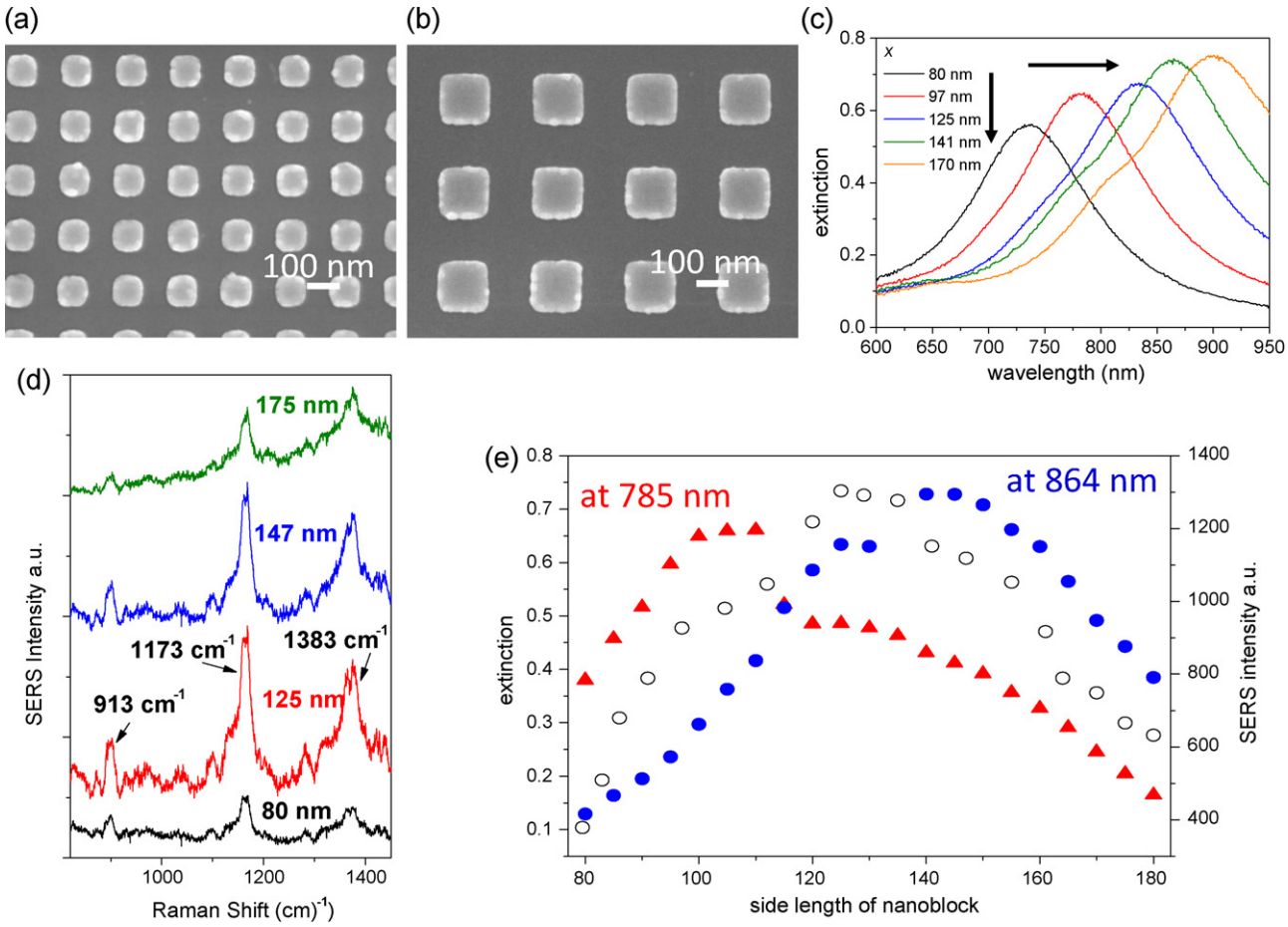


**Fig. 2.** SEM images of gold nanoblocks with side lengths of 90 nm (a) and 160 nm (b). (c) Extinction spectra of gold nanoblocks with various side lengths. (d) Stokes Raman scattering spectra of the crystal violet molecule obtained using gold nanoblocks. (e) The block size dependence of the extinction values at incident (closed triangle) and Stokes Raman scattering (closed circle) wavelengths, and the block size dependence of SERS intensity at 1173 $cm^{-1}$ in Stokes Raman scattering (open circle).

of the crystal violet molecules, respectively [68]. Significantly, the SERS intensity of each band differs for different gold nanoblock sizes. The highest SERS intensity in Stokes Raman scattering was obtained using gold nanoblocks with a side length of 125 nm. These results were inferred to be due to the difference in the enhancement factor at the wavelengths of both incident light and Raman scattering light because the plasmon resonance band is shifted by changes in block size, as shown in Fig. 2(c).

Fig. 2(e) shows the dependence of the extinction values on block size at the incident (red circle) and Stokes Raman scattering (blue circle) wavelengths. The extinction values at the incident and Raman scattering wavelengths showed maximum values for gold nanoblocks of 110-nm and 140-nm side lengths, respectively. The block-size dependence of SERS intensity at 1173 $cm^{-1}$ in Stokes Raman scattering is also shown in Fig. 2(e) (open circle). In the present study, the Raman band with a shift at 1173 $cm^{-1}$ (ring C–H out-of-plane bending) was selected to show the block-size dependence of SERS intensity. The 1173 $cm^{-1}$ band in the Stokes Raman was 864 nm with a 785-nm-wavelength laser as the excitation source for SERS measurements. As shown in Fig. 2(e), the SERS intensity exhibited peaks for nanoblocks with side lengths of 125 and 129 nm. The nanoblock size showing peak of SERS intensity in Fig. 2(e) indicates middle between two block sizes exhibiting maximum extinction values at incident and Stokes Raman scattering wavelengths. This result supports the conclusion that SERS intensity is determined by the enhancement factor at the incident light wavelength as well as the Raman scattering wavelength, as expressed in EM theory on SERS [69]. Thus, EM field enhancement effects on SERS have been elucidated using precisely fabricated gold nanoblocks. The effective tuning of the plasmon resonance band coupled to both incident light and scattered light is needed to obtain relatively large SERS intensity based on EM field enhancement effects.

### 2.2. Two-photon polymerization on gold nanoparticles

The EM field enhancement effects induced by metallic nanostructures also promote non-linear photochemical reactions. Tsuboi et al. demonstrated that the two-photon, ring-opening photochromic reaction of a diarylethene (DE) derivative can be driven by irradiation from weak, near-infrared continuous-wave laser light in the presence of gold nanoparticles [70]. Nishi et al. also showed that the one photon photochromic reaction of a DE derivative conjugated by gold nanoparticles via polymer chains proceeded efficiently due to the EM field enhancement effects localized on the gold nanoparticles [71]. As an exception to these photochromic reactions, two-photon photopolymerization on gold nanostructures have been reported by a number of researchers [72–74]. As one example, we describe here the study of a two-photon photopolymerization that is spatially promoted by near-field enhancement effects localized on gold nanoblocks [75]. The results of this study show a qualitative resemblance to the photopolymerization patterns induced in a commercial SU-8 photoresist by optical, near-field surface plasmons local-

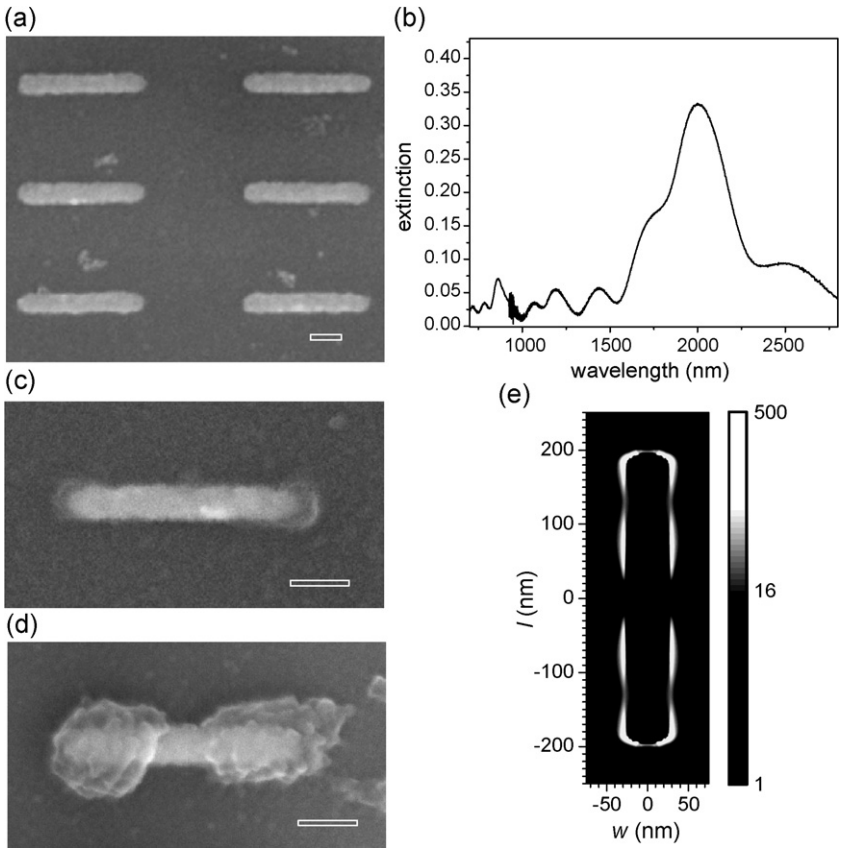


**Fig. 3.** (a) A SEM image of a periodic array of 55 nm ($w$) × 385 nm ($l$) × 32 nm ($h$) gold nanoblocks. (b) An extinction spectrum of nanoblock ensembles measured after coating with SU-8. SEM images of gold nanoblocks after exposure and development for different exposure doses, namely, $2.6 \times 10^3$ W/cm$^2$ for 1200 s (c) and $7.7 \times 10^3$ W/cm$^2$ for 120 s (d). (e) The near-field pattern calculated at a wavelength of 800 nm (log scale).

ized on rectangular gold nanoblocks. Fig. 3(a) shows a SEM image of rectangular gold nanoblocks of size 55 nm ($w$) × 385 nm ($l$) × 32 nm ($h$). The structures were spin-coated with thin films of epoxy-based negative photoresist SU-8 (MicroChem. Corp.) and subsequently irradiated by pulses from a femtosecond Ti:sapphire laser (Tsunami, Spectra Physics) with a pulse duration of 120 fs, a central wavelength of 800 nm, a repetition rate of 82 MHz, and a linear polarization parallel to the long axes of the nanoblocks (L-mode). Fig. 3(b) shows the optical extinction spectra of the LP modes for nanoblocks immersed in SU-8. The main extinction band associated with a dipolar LP mode is centered at a wavelength of 2010 nm. At shorter wavelengths, several other peaks can be seen, with the most prominent one centered at a wavelength of 830 nm. These bands represent multipolar LP modes of the nanoblocks.

Fig. 3(c) and (d) shows SEM images of gold nanoblocks irradiated with different exposure doses. The lowest detectable dose is achieved in Fig. 3(c), which is evidenced by the small amount of polymerized SU-8 near the tips of the nanoblock and its bare middle section. SEM images in Fig. 3(d) illustrate the effect of a gradual dose increase, which is achieved by approximately tripling the average irradiance and prolonging the exposure time at the same irradiance level. These images indicate that the evidence of SU-8 first emerges near the tips of the nanoblocks and then gradually spreads to fill their middle sections. The shapes of the polymerized SU-8 regions should resemble the distribution of the near-field intensity, $I^2 = |E|^4$, in the case of two-photon absorption (TPA). Fig. 3(e) shows the near-field intensity profile on the gold nanoblocks as calculated by a FDTD simulation; it depicts $I^2$ dependence to reflect the TPA nature of the photoexcitation. At higher exposure doses, photopolymerization near the tip is already saturated and occurs mainly in the surrounding regions that are characterized by lower TPA exposure levels. As shown in Fig. 3(e), constant TPA exposure lines form a multipolar pattern at lower exposure levels, which is somewhat similar to the photopolymerization images in Fig. 3(d). Thus, a two-photon photochemical reaction that was spatially promoted by near-field enhancement effects localized on gold nanoblocks was successfully demonstrated [75].

### 2.3. Plasmon-assisted photocurrent generation from visible to near-infrared wavelengths

To construct a plasmon-assisted photocurrent generation system that responds to visible to near-infrared wavelengths, gold nanoblocks exhibiting LSP resonance were fabricated on n-type $TiO_2$ single crystals (0.05 wt% niobium doped). Fig. 4(a) shows SEM images of the gold nanoblocks fabricated on the substrate. The substrate dimensions were 110 nm × 240 nm × 40 nm. These dimensions were designed to result in horizontal and vertical structural periods of 200 and 300 nm, respectively. Gold nanoblocks were fabricated within an area of 2.5 mm × 2.5 mm on the $TiO_2$ substrate. A $TiO_2$ single crystal with gold nanoblocks was used as a working electrode in the photoelectrochemical measurement system. In this system, light was irradiated on the 2 mm $\phi$ area of the working electrode corresponding to the area of gold nanoblocks, and the 2 mm $\phi$ electrode was immersed in an aqueous electrolyte solution (KCl or $KClO_4$, 0.1 M). The incident photon-to-photocurrent efficiency (IPCE) values of the photocurrent were obtained by dividing the number of generated electrons by the number of irradiated photons. Fig. 4(b) presents the extinction spectra for gold nanoblocks prepared on the $TiO_2$ single crystal in an aqueous electrolyte solution. A broad LSP band

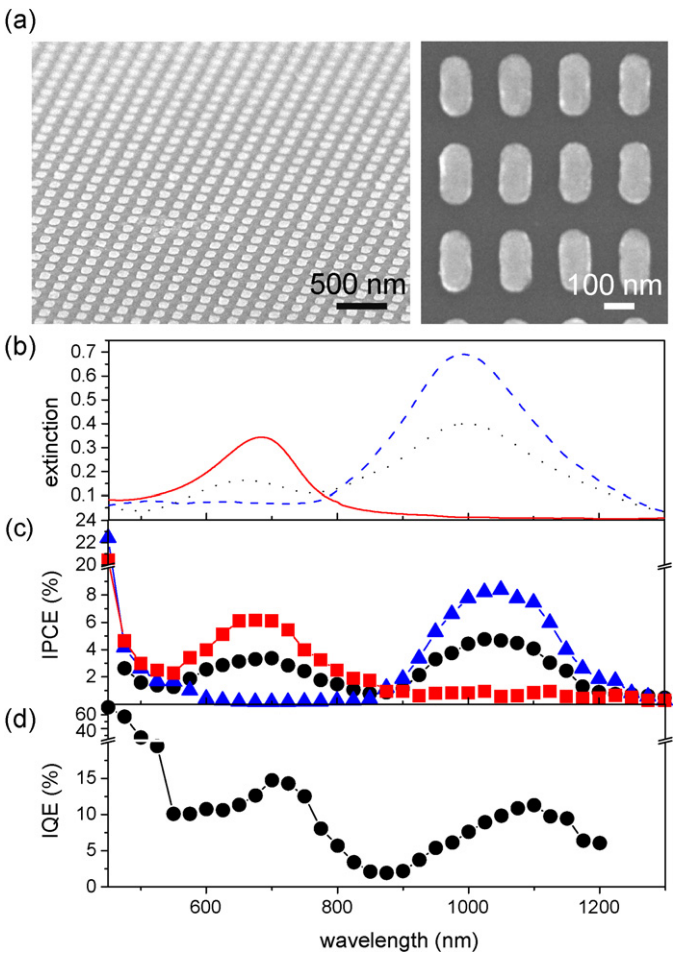


**Fig. 4.** (a) A SEM image of the gold nanoblocks on a $TiO_2$ substrate. The figure on the right side shows a SEM image taken from directly above the substrate. The figure on the left side shows a SEM image of the same substrate tilted by 75 degrees. (b) Extinction spectra of the gold nanoblocks in water. Dashed line: under irradiation by non-polarized light; solid and broken lines: T mode and L mode, respectively, under irradiation with linearly polarized light. (c) Photoelectric conversion efficiency of the action spectrum measured at each wavelength with monochromatic light (wavelength interval: 10 nm) irradiated with a monochromator. closed circle: non-polarized light; closed square polarized light in T-mode; closed triangle: polarized light in L-mode. (d) Internal quantum efficiency obtained by standardizing the photoelectric conversion efficiency.

was observed around the wavelengths of 650 nm (T-mode) and 1000 nm (L-mode), which can be selectively excited by controlling the orientation of the linear polarization of the incident light. An extinction spectrum measured under non-polarized conditions is also shown (black curve). The *I–V* measurement was conducted in the dark as well as under light irradiation of wavelengths 500–1300 nm. An anodic photocurrent was observed at positive potentials above −0.3 V (data not shown here). We confirmed that the stability of the photocurrent was continuous during the entire photocurrent measurement, corresponding to 200 h. According to the results on the photocurrent spectrum using linear polarization (Fig. 4(c)), the incident photon-to-photocurrent efficiency (IPCE) values of the photocurrent were 6.3% and 8.4% for the LSP bands for T mode at 650 nm and L mode at 1000 nm, respectively. Notably, no photocurrent was observed at the $TiO_2$ single crystal under light irradiation with a wavelength of 450 nm or longer without the presence of the gold nanoblocks. This demonstrates that electron transfer from the gold nanoblocks to the $TiO_2$ single crystal substrate is induced by LSP excitation. Of even greater significance, this $TiO_2$ single crystal with gold nanoblocks allows the generation of a photocurrent by irradiation with infrared light at longer wavelengths from 800 to 1300 nm. This system is superior to that of a previously reported photovoltaic cell [76–78] because a photocurrent can be produced in response to quite a wide range of the solar spectrum, ranging from visible radiation to infrared light, using simple gold nanoblocks, and this system does not require different dye-sensitizers with spectral absorbances at different wavelengths or semiconductors with different band gaps, as in a tandem solar cell.

The photocurrent produced from a monochromatic photon flux can be expressed by the internal quantum efficiency (IQE), which is the number of electrons injected into the conduction band of $TiO_2$ per photon interacting with the gold nanoblocks. The IQE is calculated by correcting the IPCE based on photons interacting with the gold nanoblocks using IQE = IPCE/$\eta$, where $\eta$ is the probability of interaction between the photons and gold nanoblocks. Therefore, $\eta$ can be expressed by (*total photon flux* − *transmitted photon flux*)/*total photon flux*. Fig. 4(d) shows the IQE values plotted against the wavelength of incident monochromatic light. As clearly observed in this figure, this photoelectric conversion system demonstrates that the quantum efficiency near the LSP band of the T mode and L mode depends on the wavelength, and there are local maximum values for each. In an IQE measurement for a general photoelectrochemical system, IQE does not depend on the wavelength that corresponds to the absorption spectrum of the sensitizer driving the photoelectron transfer [79]. This result suggests that the photo induced electron transfer from the gold nanoblocks to the $TiO_2$ resulting from excitation of the LSPs is promoted by electromagnetic field enhancement effects.

We found that our system is characterized by a highly efficient photocurrent without the inclusion of certain electron donors. However, the photocurrent was stable for more than 200 h when only the electrolyte solution (aq. KCl or $KClO_4$) was used in the photoelectrochemical measurement, suggesting that hydroxide ions or water molecules may potentially act as donors that provide electrons into the d-band holes. This process is assisted by the LSP excitation in the present system. We speculate that these results suggest that interband transition from the d-bands to the sp-conduction band is promoted, and pairs of an excited electron and electron hole should form around the interface between the gold nanoblocks and $TiO_2$; however, the hole should be trapped at the $TiO_2$ surface states when the LSPs are excited by light with wavelengths shorter than 700 nm [80]. The density of states in the d-bands of gold is known to decrease from the Fermi level of around 1.8 eV [81,82]. Therefore, the probability of an interband transition from d-bands to the sp-conduction band when excited by wavelengths from 700 to 1300 nm is considered very low. However, the intense optical near-field that is locally augmented by plasmonic enhancement effects at the nanoblock tips may assist in the electronic excitation of gold with near infrared wavelengths and result in successful electron transfer from the gold nanoblocks to the conduction band of the $TiO_2$. Thus, a multi-electron transfer process via oxidation of hydroxide ions and/or water molecules will contribute to photocurrent generation.

## 3. Conclusions

In this review, recent studies elucidating the strong coupling between a photon and a molecule and its application to photochemical reactions are discussed. The fabrication of gold nanoblocks using an advanced nanoprocessing technique is described, and the resolution of the gold nanoblocks was successfully elucidated

based on measurements of their optical properties. Electromagnetic field enhancement effects localized on the gold nanoblocks were also elucidated using surface-enhanced Raman scattering spectroscopy. This study emphasizes the importance of coupling efficiency between LSP resonance and incident or Raman scattered light. Two-photon polymerization of a negative photoresist, which was spatially promoted by near-field enhancement effects localized on the gold nanoblocks, was clearly demonstrated. Thus, gold nanostructures may be utilized as photochemical reaction fields that promote strong, photon-efficient coupling between photons and molecules. This concept was applied to plasmonic, photoelectric conversion from visible to near-infrared wavelengths using electrodes in which gold nanoblocks were elaborately arrayed on the surface of a single $TiO_2$ crystal. Significantly, the results of this study indicate that the photocurrent was stable for more than 200 h without adding the donors, which suggests the possibility that water molecules can act as donors that provide electrons to the d-band holes assisted by the LSP excitation. Therefore, it can be deduced that four-electron oxidation of water molecules can be expected. This oxidation is important because there is a possibility that the system can behave as an artificial photosynthesis system using irradiation with near-infrared light.

## Acknowledgments

The authors are very grateful and indebted to Prof. Vygantas Mizekis (Shizuoka University), Dr. Naoki Murazawa, Dr. Yoshiaki Nishijima, Dr. Yukie Yokota, Prof. Keiji Sasaki, Prof. Kei Murakoshi (Hokkaido University), Prof. Haruo Inoue (Tokyo Metropolitan University), and Prof. Akihito Imanishi (Osaka University) for their experimental and theoretical contributions and fruitful discussions. This work was supported by funding from the Ministry of Education, Culture, Sports, Science, and Technology of Japan: KAKENHI Grant-in-Aid for Scientific Research on the Priority Area "Strong Photon-Molecule Coupling Fields" (No. 470 (No. 19049001)), KAKENHI Grant-in-Aid (No. 20710068), and Grants-in-Aid from Hokkaido Innovation through Nanotechnology Support (HINTS). K.U. also acknowledges the JST PRESTO program.

## References

[1] S. Owa, H. Nagasaka, J. Micro-Nanolith. Membr. 3 (2004) 97–103.
[2] S. Tarutani, H. Tsubaki, S. Kanna, J. Photopolym. Sci. Technol. 21 (2008) 685–690.
[3] H. Kojima, N. Nakatsubo, K. Kikuchi, S. Kawahara, Y. Kirino, H. Nagoshi, Y. Hirata, T. Nagano, Anal. Chem. 70 (1998) 2446–2453.
[4] T. Nagai, K. Ibata, E.S. Park, M. Kubota, K. Mikoshiba, A. Miyawaki, Nat. Biotechnol. 20 (2002) 87–90.
[5] M. Havaux, R.J. Strasser, H. Greppin, Photosynth. Res. 27 (1991) 41–55.
[6] H. Inoue, S.S. Funyu, Y. Shimada, S. Takagi, Pure Appl. Chem. 77 (2005) 1019–1033.
[7] A. Fujishima, K. Honda, Nature 238 (1972) 37–38.
[8] M.R. Hoffmann, S.T. Martin, W.Y. Choi, D.W. Bahnemann, Chem. Rev. 95 (1995) 69–96.
[9] B. O'Regan, M. Grätzel, Nature 353 (1991) 737–740.
[10] M.K. Nazeeruddin, A. Kay, I. Rodicio, R. Humphrybaker, E. Muller, P. Liska, N. Vlachopoulos, M. Grätzel, J. Am. Chem. Soc. 115 (1993) 6382–6390.
[11] R.A. Marcus, J. Chem. Phys. 24 (1956) 966–978.
[12] N. Mataga, T. Okada, N. Yamamoto, Bull. Chem. Soc. Jpn. 39 (1966) 2562.
[13] T. Förster, Ann. Phys. 2 (1948) 55–75.
[14] D.L. Dexter, Phys. Rev. 108 (1957) 630–633.
[15] K. Ueno, S. Juodkazis, T. Shibuya, Y. Yokota, V. Mizeikis, K. Sasaki, H. Misawa, J. Am. Chem. Soc. 130 (2008) 6928–6929.
[16] A. Salomon, C. Genet, T.W. Ebbesen, Angew. Chem. Int. Ed. 48 (2009) 8748–8751.
[17] K. Ueno, S. Juodkazis, T. Shibuya, Y. Yokota, V. Mizeikis, K. Sasaki, H. Misawa, J. Phys. Chem. C 113 (2009) 11720–11724.
[18] C. Deeb, R. Bachelot, J. Plain, A.-L. Baudrion, S. Jradi, A. Bouhelier, O. Soppera, P.K. Jain, L. Huang, C. Ecoffet, L. Balan, P. Royer, ACS Nano 4 (2010) 4579–4586.
[19] K. Ueno, S. Takabatake, Y. Nishijima, V. Mizeikis, Y. Yokota, H. Misawa, J. Phys. Chem. Lett. 1 (2010) 657–662.
[20] Y. Nishijima, K. Ueno, Y. Yokota, K. Murakoshi, H. Misawa, J. Phys. Chem. Lett. 1 (2010) 2031–2036.
[21] S. Yamazaki, A. Mase, K. Urata, K. Shibata, H. Shinohara, S. Nagayama, M. Abe, T. Hamatani, K. Suzuki, IEEE Electr. Device Lett. 5 (1984) 315–318.
[22] Y. Tian, T. Tatsuma, J. Am. Chem. Soc. 127 (2005) 7632–7637.
[23] K.F. Yu, Y. Tian, T. Tatsuma, Phys. Chem. Chem. Phys. 8 (2006) 5417–5420.
[24] Y.-Y. Yu, S.-S. Chang, C.-L. Lee, C.R.C. Wang, J. Phys. Chem. B 101 (1997) 6661–6664.
[25] R. Jin, Y. Cao, C.A. Mirkin, K.L. Kelly, G.C. Schatz, J.G. Zheng, Science 294 (2001) 1901–1903.
[26] N.R. Jana, L. Gearheart, C.J. Murphy, Chem. Commun. (2001) 617–618.
[27] F. Kim, J.H. Song, P. Yang, J. Am. Chem. Soc. 124 (2002) 14316–14317.
[28] Y. Niidome, K. Nishioka, H. Kawasaki, S. Yamada, Chem. Commun. (2003) 2376–2377.
[29] E. Prodan, P. Nordlander, N.J. Halas, Nano Lett. 3 (2003) 1411–1415.
[30] C.M. Doudna, M.F. Bertino, F.D. Blum, A.T. Tokuhiro, D. Lahiri-Dey, S. Chattopadhyay, J. Terry, J. Phys. Chem. B 107 (2003) 2966–2970.
[31] S.C. Yang, H. Kobori, C.L. He, M.H. Lin, H.Y. Chen, C.C. Li, M. Kanehara, T. Teranishi, S. Gwo, Nano Lett. 10 (2010) 632–637.
[32] G. Laurent, N. Félidj, J. Aubard, G. Lévi, J.R. Krenn, A. Hohenau, G. Schider, A. Leitner, F.R. Aussenegg, J. Chem. Phys. 122 (2005) 011102–11111.
[33] T.D. Corrigan, S.H. Guo, H. Szmacinski, R.J. Phaneuf, Appl. Phys. Lett. 88 (2006) 101112–101121.
[34] K. Ueno, S. Juodkazis, M. Mino, V. Mizeikis, H. Misawa, J. Phys. Chem. C 111 (2007) 4180–4184.
[35] P.K. Jain, W. Huang, M.A. El-Sayed, Nano Lett. 7 (2007) 2080–2088.
[36] K. Ueno, V. Mizeikis, S. Juodkazis, K. Sasaki, H. Misawa, Opt. Lett. 30 (2005) 2158–2160.
[37] Y. Yokota, K. Ueno, V. Mizeikis, S. Juodkazis, K. Sasaki, H. Misawa, J. Nanophotonics 1 (2007) 011594–11601.
[38] K. Ueno, Y. Yokota, S. Juodkazis, V. Mizeikis, H. Misawa, Curr. Nanosci. 4 (2008) 232–235.
[39] M.B. Mohamed, K.Z. Ismail, S. Link, M.A. El-Sayed, J. Phys. Chem. B 102 (1998) 9370–9374.
[40] S. Link, M.B. Mohamed, M.A. El-Sayed, J. Phys. Chem. B 103 (1999) 3073–3077.
[41] O. Wilson, G.J. Wilson, P. Mulvaney, Adv. Mater. 14 (2002) 1000–1004.
[42] H. Kuwata, H. Tamaru, K. Esumi, K. Miyano, Appl. Phys. Lett. 83 (2003) 4625–4627.
[43] H. Tamaru, H. Kuwata, H.T. Miyazaki, K. Miyano, Appl. Phys. Lett. 80 (2002) 1826–1831.
[44] W. Rechberger, A. Hohenau, A. Leitner, J.R. Krenn, B. Lamprecht, F.R. Aussenegg, Opt. Commun. 220 (2003) 137–141.
[45] K.-H. Su, Q.-H. Wei, X. Zhang, J.J. Mock, D.R. Smith, S. Schultz, Nano Lett. 3 (2003) 1087–1090.
[46] P. Nordlander, C. Oubre, E. Prodan, K. Li, M.I. Stockman, Nano Lett. 4 (2004) 899–903.
[47] T. Atay, J.-H. Song, A.V. Nurmikko, Nano Lett. 4 (2004) 1627–1631.
[48] S. Link, M.A. El-Sayed, J. Phys. Chem. B 103 (1999) 8410–8426.
[49] C. Sönnichsen, T. Franzl, T. Wilk, G. von Plessen, J. Feldmann, O. Wilson, P. Mulvaney, Phys. Rev. Lett. 88 (2002) 077402–77411.
[50] K.L. Kelly, E. Coronado, L.L. Zhao, G.C. Schatz, J. Phys. Chem. B 107 (2003) 668–677.
[51] K. Ueno, S. Juodkazis, V. Mizeikis, K. Sasaki, H. Misawa, J. Am. Chem. Soc. 128 (2006) 14226–14227.
[52] Y. Inouye, S. Kawata, Opt. Lett. 19 (1994) 159–161.
[53] A. Bouhelier, M.R. Beversluis, L. Novotny, Appl. Phys. Lett. 83 (2003) 5041–5043.
[54] O.P. Varnavski, M.B. Mohamed, M.A. El-Sayed, T. Goodson III, J. Phys. Chem. B 107 (2003) 3101–3104.
[55] K. Imura, T. Nagahara, H. Okamoto, J. Am. Chem. Soc. 126 (2004) 12730–12731.
[56] H. Wang, C.S. Levin, N.J. Halas, J. Am. Chem. Soc. 127 (2005) 14992–14993.
[57] K. Ueno, S. Juodkazis, V. Mizeikis, K. Sasaki, H. Misawa, Adv. Mater. 20 (2008) 26–30.
[58] K. Imura, T. Nagahara, H. Okamoto, J. Phys. Chem. B 109 (2005) 13214–13220.
[59] A. Hohenau, J.R. Krenn, J. Beermann, S.I. Bozhevolnyi, S.G. Rodrigo, L. Martin-Moreno, F. Garcia-Vidal, Phys. Rev. B 73 (2006) 155404–155411.
[60] E.M. Kim, S.S. Elovikov, T.V. Murzina, A.A. Nikulin, O.A. Aktsipetrov, Phys. Rev. Lett. 95 (2005) 227402–227411.
[61] S. Kim, J. Jin, Y.-J. Kim, I.-Y. Park, Y. Kim, S.-W. Kim, Nature 453 (2008) 757–760.
[62] D.L. Jeanmaire, R.P. Van Duyne, J. Electroanal. Chem. 84 (1977) 1–20.
[63] K. Kneipp, Y. Wang, H. Kneipp, L.T. Perelman, I. Itzkan, R.R. Dasari, M.S. Feld, Phys. Rev. Lett. 78 (1997) 1667–1670.
[64] S. Nie, S.R. Emory, Science 275 (1997) 1102–1106.
[65] Y. Sawai, B. Takimoto, H. Nabika, K. Ajito, K. Murakoshi, J. Am. Chem. Soc. 129 (2007) 1658–1662.
[66] K. Yoshida, T. Itoh, V. Biju, M. Ishikawa, Y. Ozaki, Phys. Rev. B 79 (2009), 085419-1-6.
[67] S.A. Maier, Plasmonics: Fundamentals and Applications, Springer, New York, 2007.
[68] E.J. Liang, X.L. Ye, W. Kiefer, J. Phys. Chem. A 101 (1997) 7330–7335.
[69] Y. Yokota, K. Ueno, H. Misawa, Small 7 (2011) 252–258.
[70] Y. Tsuboi, R. Shimizu, T. Shoji, N. Kitamura, J. Am. Chem. Soc. 131 (2009) 12623–12627.
[71] H. Nishi, T. Asahi, S. Kobatake, J. Phys. Chem. C 113 (2009) 17359–17366.
[72] C. Hubert, A. Rumyantseva, G. Lérondel, J. Grand, S. Kostcheev, L. Billot, A. Vial, R. Bachelot, P. Royer, S.H. Chang, S.K. Gray, G.P. Wiederrecht, G.C. Schatz, Nano Lett. 5 (2005) 615–619.

[73] A. Sundaramurthy, P.J. Schuck, N.R. Conley, D.P. Fromm, G.S. Kino, W.E. Moerner, Nano Lett. 6 (2006) 355–360.
[74] H. Ahrach, R.I. Bachelot, A. Vial, G. Lerondel, J. Plain, P. Royer, O. Soppera, Phys. Rev. Lett. 98 (2007) 107402–107411.
[75] N. Murazawa, K. Ueno, V. Mizeikis, S. Juodkzis, H. Misawa, J. Phys. Chem. C 113 (4) (2009) 1147–1149.
[76] M.K. Nazeeruddin, P. Pechy, M. Grätzel, Chem. Commun. 18 (1997) 705–706.
[77] Y.B. Cao, J. Zhang, M. Wang, R. Li, P. Wang, S.M. Zakeeruddin, M. Grätzel, Nat. Mater. 7 (2008) 626–630.
[78] M. Grätzel, Nature 414 (2001) 338–344.
[79] E.W. McFarland, J.A. Tang, Nature 421 (2003) 616–618.
[80] O.I. Micic, Y.N. Zhag, K.R. Cromack, A.D. Trifunac, M.C. Thurnauer, J. Phys. Chem. 97 (1993) 7277–7283.
[81] P.B. Johnson, R.W. Christy, Phys. Rev. B 6 (1972) 4370–4379.
[82] N.E. Christensen, Phys. Rev. B 13 (1976) 2698–2701.